# Studies of physicochemical characteristics of organoclay with carboxydecyltriethylammonium chloride ion

Shu-Lung Kuo & Ching-Lin Ho

Published online: 24 Mar 2021.

Submit your article to this journal 

Article views: 48

View related articles 

View Crossmark data

Taylor & Francis
Taylor & Francis Group

Check for updates

# Studies of physicochemical characteristics of organoclay with carboxydecyltriethylammonium chloride ion

Shu-Lung Kuo and Ching-Lin Ho

Department of Technology Management, The Open University of Kaohsiung, Kaohsiung City, Taiwan

## ABSTRACT

This study used the soil representative of Taitung in Taiwan, Santai (St) series soil, as the catalyst carrier and exchanged arboxydecyltriethylammonium chloride (CDTEA) onto it through ion exchange, forming nano-level St-CDTEA organoclay via surface modification and high-temperature sintering. The physical and chemical properties of the St-CDTEA organoclay were then studied via a series of physical and chemical experiments.First, an analysis of the basic properties of St series soil shows that it does not have a high organic matter content because it is affected by either rainfall erosion or intensive farming, which causes a decrease in organic matter after it is consumed or lost. The Fourier-transform infrared spectroscopy (FT-IR) analysis suggests that compared with the unmodified St series soil, C-H bonds are found between 2900 cm-1 and 2850 cm-1 and COOH bond around 1750 cm-1 in St-CDTEA organoclay. A field emission scanning electron microscope (FE-SEM) analysis shows the formation of a crystal structure on the surface of the St-CDTEA organoclay because St series soil contains a larger amount of smectite and the structure of the St-CDTEA organoclay absorbs a significant amount of CDTEA molecules (the molecular structure of CDTEA contains three ethyls) after high-temperature sintering.

## 1. Introduction

The clay minerals' properties, high cation exchange capacity, swelling property and high surface areas make clays such as smectite favorable materials to be widely used as rheology control reagents, sorbents in pollution prevention and environmental remediation. Their potentials have been tremendously expanded by ion-exchange of organo cations with interlamellar exchangeable metal cations to impart hydrophobic properties. When long-chain alkylammonium cations are used, a hydrophobic partition medium within the clay interlayer can form and function analogously to a bulk organic phase. Studies have shown that replacing the inorganic exchangeable cations of clay minerals with organic cations can result in a greatly enhanced capacity of these materials to remove organic contaminants (Xi et al. 2005a; Ma et al. 2019a). Organoclay-based nanocomposites exhibit a remarkable improvement in properties. These improvements include increased strength and heat resistance, decreased gas permeability and flammability, and increased biodegradability (Xi, He, and Frost 2005b; Spadavecchia et al. 2014). Investigation of different surfactant environments, surfactant configurations, vibrational spectroscopy and morphology of organoclay is of great importance in this project. For instance, XRD has proven a useful technique for the study of surfactant configurations between clay layers via d001 basal spacing (He et al. 2006; Li et al. 2017); thermogravimetric analysis (TG) provides a tool for the identification of different surfactant environments and structure arrangements and for revealing of their thermal and structural stabilities (Carmody et al. 2005; Gao et al. 2015). Scanning and transmission electron microscopy (SEM and TEM) are used to collect detailed information on the morphology. Infrared spectroscopy is a powerful tool for the study of the bonding mechanisms on a molecular scale which provides structural information about organoclays (He et al. 2006; Guégan 2019).

When nanocomposites are used to treat pollutants in various media, they help to degrade pollutants in wastewater, air, wastes, and soil completely via oxidation. However, more time and effort are required to separate media treated with nanocomposites. During practical applications, general nanocomposites are immobilized to solve the concerns of repeated use and separation. Basis materials generally include: glass, ceramic tile, metal, filters, fiber, and plastic. Because of the non-adherence of nanocatalysts, an adhesive (such as epoxy resin, PVC, or waterproof lacquer paint) is often needed for catalyst immobilization. Although nanocomposites may break some basic materials or binders, separation between nanocomposites and basis materials is required and a proper adhesive shall be used (Kuo and Wu 2014a; Kushwaha et al. 2015).

On the other hand, organoclay materials are defined as hybrid materials resulting from the association of clay minerals (swelling ones such as montmorillonite (Mt), vermiculite, and saponite) with surfactants and/or other various organic compounds (He et al. 2014). With the incorporation of the surfactants in their internal structure through different chemical and physical processes, the obtained materials combine a large specific surface and a hydrophobic behavior, enhancing the applications of clay minerals in various fields. A large volume of the extant research work has focused on and pointed out the use of organoclays as

---

reinforcers in polymer nanocomposites, starting materials for photophysical films, rheological agents, and as adsorbents for organic pollutants in soil and aquatic environments (Ugochukwu and Fialips 2017; Li et al. 2015).

This study aims to use the soil representative of Eastern Taiwan as the main carrier to exchange CDTEA onto the carrier via ion exchange, forming nano-level St-CDTEA organoclay with catalytic capability. The physical and chemical properties of the St-CDTEA organoclay are studied using various instruments. In the future, the results can be applied to the absorption of, and catalytic reactions for, inorganic and organic pollutants, respectively.

## 2. Materials and methods

### 2.1. Sources of test soil

This study selects Taiwanese soil from Taitung County-Santai (St) series soil as the sampling soil sample. It is a black soil formed by a mixture of igneous rock and mud rock. St series soil was collected and dried at room temperature for two days. It was then ground using glass bottles after impurities were removed. After running through 2 mm sieves, the ground soil was stored in boxes, pending an analysis of its basic properties.

### 2.2. Synthesis and identification of CDTEA

We mixed 2 g 11-bromoundecanoic acid (white crystal powder) dissolved in 0.1 N sodium carbonate solution at 50 mL, with 0.1 N triethylamine at 50 mL with equivalent mole concentration, heating reflux with stirring until solution became clear. After acidifying product solution by hydrochloric acid to pH 2–3, place still to crystallize overnight. Recrystallize with acetone and dry to complete.

### 2.3. Preparation of St-CDTEA organoclay

Take 0.5 g St series soil and add 30 ml of the CDTEA solution with a value equivalent to 0.75 times the CEC value. Continuously heat it up and oscillate it in a water bath at 80°C for 24 h. Separate a solid from the liquid using a high-speed centrifuge at 20,000 rpm. Inspect whether the supernatant has white sediment after centrifugation using $AgNO_3$, to ensure that the chloride ions have been completely removed. After freeze-drying the modified St-CDTEA organoclay, grind it using an agate mortar and then store it. Conduct the subsequent characteristic analysis and absorption test.

### 2.4. Verification of the function group of fourier-transform infrared spectroscopy (FT-IR)

The principle of FT-IR is using rotations or vibrations of molecules to absorb radiation at the same frequency (Sun et al. 2020). The fingerprint and Eigen areas in FT-IR can help to determine the existence of isomorphous replacement structure or organic molecules in the St-CDTEA organoclay.

Put the St-CDTEA organoclay and KBr powders in an oven. After heating them up and drying them for 48 hours, mix them evenly in a 1:10 ratio, and then grind the mixture with an agate mortar. Use a hydraulic press to press the mixture at 10 tons/hour, making it into a transparent foil. Put the foil in a spectrometer and perform an analysis with a scan range of 4,000 $cm^{-1}$ to 400 $cm^{-1}$.

### 2.5. X-ray diffraction analysis (XRD Analysis)

The XRD analysis is conducted using an x-ray diffractometer (Rigaku RINT-2000). With CuKa as the light source, an analysis of the crystal patterns of the St-CDTEA organoclay is performed to learn the spacing of layers of materials. The x-ray wavelength produced is 1.5418 °$A$; the operating current during testing is 10 mA; the voltage is 20 kV; the scanning speed is 5 deg/min; and the scanning angle is $2\theta = 2 \sim 40°$.

### 2.6. Field emission scanning electron microscope (FE-SEM) analysis of St Series soil and St-CDTEA organoclay

With a scanning electron microscope (SEM), this study observes the size of St series soil and St-CDTEA organoclay and their distribution. The model in use is JEOL-6330, and its emitting energy comes from the field emission filament with high space and energy resolution (Doan et al. 2019).

### 2.7. Analyzing the converter dust using a thermogravimetric analyzer (TGA)

A thermogravimetric analyzer is mostly used to measure the pyrolysis temperature and composition of materials. This study used a dynamic TGA (Dynamic TGA 2950) to determine the weight loss of the sample under different temperatures. To analyze the sample, we placed 10–20 mg of dried sample (St-CDTEA organoclay) in a platinum crucible and heated it at room temperature (about 25°C), with the air as the oxidizer. The temperature of the sample increased at a rate of 10°C per min until finally reaching the target temperature of 1000°C. After reaching the target temperature, the sample was analyzed for its weight reduction rate and induced degradation rate.

## 3. Results and discussion

### 3.1. An analysis of the basic properties of St series soil

Table 1 shows the results of an analysis of the basic properties of St series soil and St-CDTEA organoclay. As shown in the table, St series soil is a type of mid-acid soil. The pH values of soils are affected by various external and internal factors, such as different parent materials, precipitation amounts, degrees of soil development, types of colloids contained in soils, types of ion exchange, and amounts of soluble salts. Furthermore, Table 1 indicates that St series soil does not have a high organic matter content because it is affected by either rainfall erosion or intensive farming, which causes a decrease in organic matter after it is consumed or lost. Besides, St series soil, primarily located in rainy Eastern Taiwan, is low in organic matter content, indicating that its parent material is a type of black soil

**Table 1.** An analysis of the basic properties of St series soil and St-CDTEA organoclay.

| Soil | pH | CEC (cmole/g) | Organic matter (%) | Texture Sand (%) | Silt (%) | Clay (%) |
|------|-----|---------------|---------------------|------------------|----------|----------|
| St series soil | 6.01 | 38.03 | 3.32 | 48.0 | 26.1 | 25.9 |
| St-CDTEA organoclay | – | 85.65 | – | – | – | – |

mostly consisting of igneous rock and mudstone. The color of the soil suggests that it contains humus that is hard to disintegrate. In addition, the cation exchange capacity (CEC) of a soil is always affected by its texture, types of colloids contained, and organic matter content. CEC values always increase as clay and organic matter content increase (Ugochukwu and Fialips 2017; Ma et al. 2018). As shown in the table, St series soil is a type of sandy clay loam with a CEC value of 38.03 cmole/g, which we presume to be a resulting product of clay and organic matter. In terms of St-CDTEA organoclay in Table 1, its CEC value shows a significant increase in the capacity of CDTEA-modified clay to absorb cations when compared to that of the

original St series soil. This suggests that organic matter and free oxides attached to the surface of clay minerals have been removed in the pretreatment process; the St-CDTEA organoclay thus has a higher amount of charge.

### 3.2. Results of FT-IR analysis of St series soil and St-CDTEA organoclay

Figure 1 shows the results of FT-IR analysis of CDTEA, St series soil and St-CDTEA organoclay, respectively, where C-H bonds are found between 2900 $cm^{-1}$ and 2850 $cm^{-1}$ and COOH bond around 1750 $cm^{-1}$ in St-CDTEA organoclay when compared with unmodified St series soil in Figure 1(a). However, Figure 1(b) suggests that the intensity of St series soil's absorption bands is not strong. From this result we can infer that the molecular structure of CDTEA cannot provide better positions for reaction when CDTEA is inserted into the interlayers because it contains three ethyls, thereby slightly affecting the modification effects (Carrado 2000; Doan et al. 2019; Yin et al. 2019). However, as mentioned earlier, after we modified the clay with CDTEA, adsorption peaks of bonds occurred in several positions, suggesting that C-H and COOH bonds were successfully inserted into the structure of the St-CDTEA organoclay. This result indicates that when smectite-CDTEA is adopted for the catalysis of pollutants in the future (Ma et al. 2019b), it will have enough capacity to disintegrate or attract pollutants. Our research findings are similar to those of other studies. For example, Zhu et al. (2008) proved that from FT-IR, for example, the vibration at 1198 $cm^{-1}$ corresponds to Si-O-Si- stretching mode. In surfactant-modified hydrotalcite (LDH-2), the loaded surfactants are located in both the interlayer space and the interparticle pores with a 'house of cards' structure as supported by FT-IR (Sun et al. 2020; Das et al. 2020). Moreover, factors such as temperature control when synthesizing CDTEA and the rate of adding triethylamine can affect the purity of synthesized CDTEA, which in turn affects the modification effects. This result can also be corroborated by the research findings of Kuo and Wu (2014b).

### 3.3. Results of XRD analysis

Figure 2 shows the results of XRD analysis of St series soil and St-CDTEA organoclay, respectively. As shown in Figure 2(a), a diffraction peak is found at 1.004 nm after saturating St series soil with potassium at room temperature. Diffraction peaks are found at 1.002 nm, 1.000 nm and 1.004 nm when St series soil is heated to 110°C, 350°C and 550°C, respectively, but changes in the spacing of layers are not obvious. A diffraction peak is found at 1.483 nm after saturating St series soil with
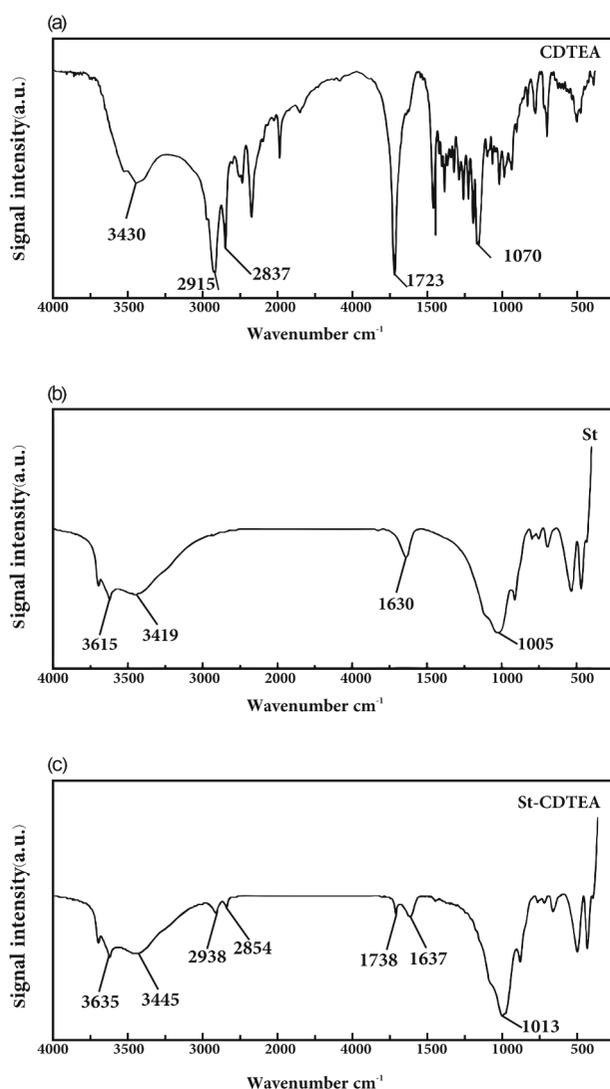


**Figure 1.** (a) FT-IR spectrum of CDTEA; (b) St series soil; (c) St-CDTEA organoclay.
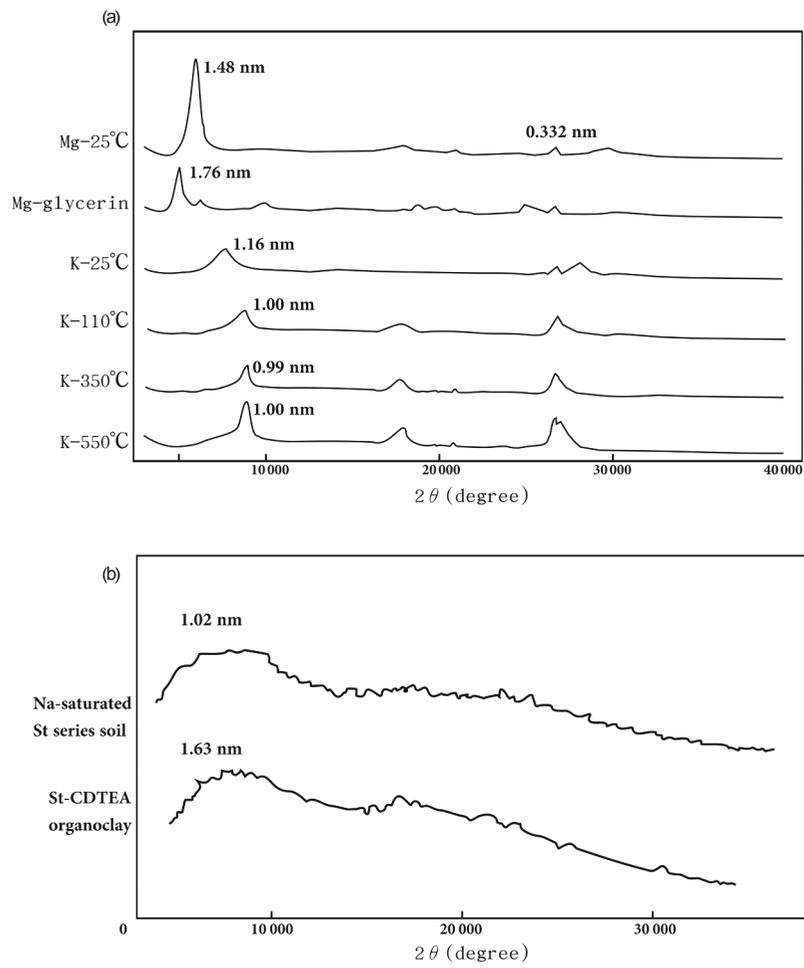
Figure 2. (a) St series soil; (b) Na-saturated St series soil and St-CDTEA organoclay.
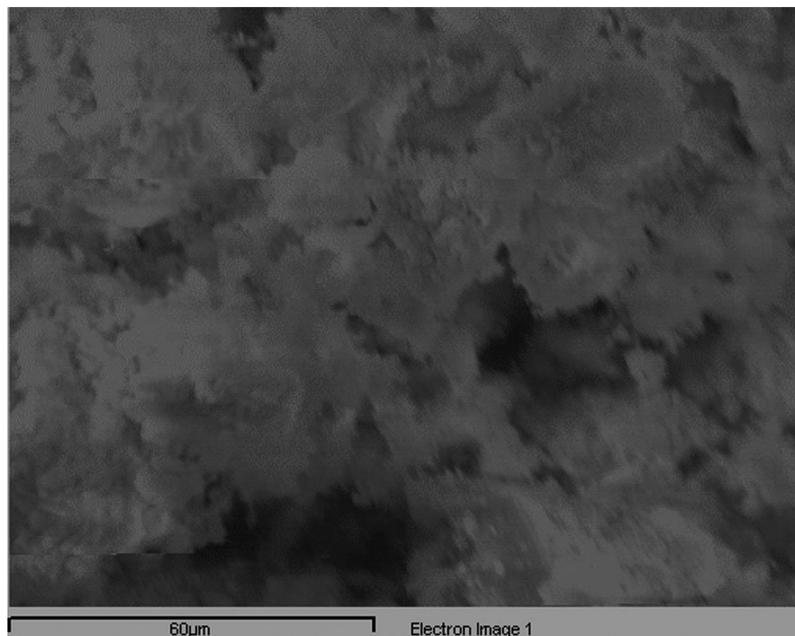


Figure 3. FE-SEM analysis of St series soil.

magnesium. The spacing of layers expands to 1.758 nm after fumigating St series soil with glycerin. From these results, we can infer that smectite is the main element of the clay of St series soil. This research finding is similar to that of Zhu et al. (2008), i.e. the Mg-Al hydrotalcite (LDH) and the only surfactant-modified hydrotalcite (LDH-2) display similar XRD patterns while both surfactant and silane-modified hydrotalcite (LDH-3) show two distinct series of reflections, corresponding to hydrotalcite and smectite-like materials, respectively (Yin et al. 2019; Yan et al. 2020). Also, in this study, diffraction peaks produced by different angles across the spectrum in Figure 2

(a) suggest that St series soil contains other mineral mixtures, such as quartz. Figure 2(b) shows that the spacing of layers for unmodified St series soil is approximately 1.02 nm, whereas that for CDTEA-modified St series soil increases to 1.44 nm, an increase by 0.42 nm. This result suggests that the way in which CDTEA is inserted into the interlayers of the clay is double-layered absorption, thereby presenting a double-layered arrangement of St-CDTEA organoclay in solid interlayers (Guégan 2019). The result of ion exchange is applicable to the formation of St-CDTEA organoclay as a catalyst; this type of ion
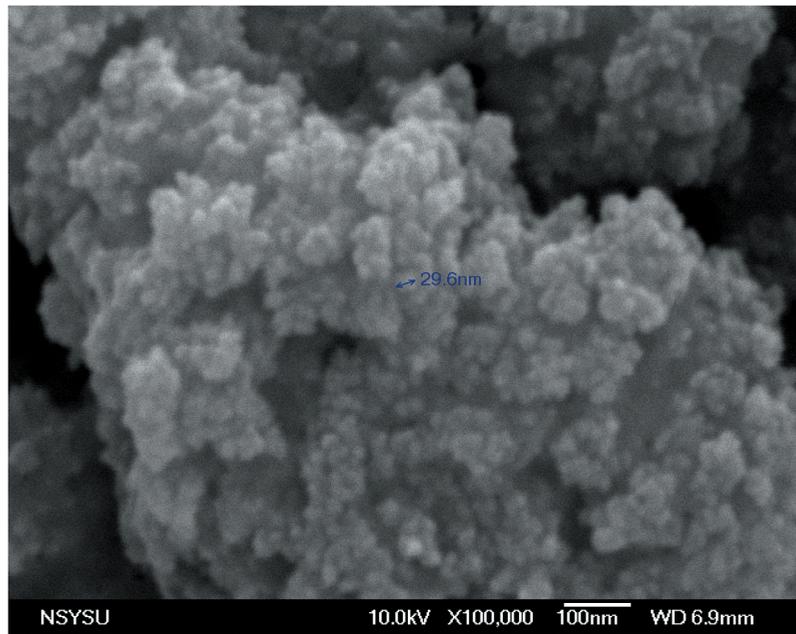


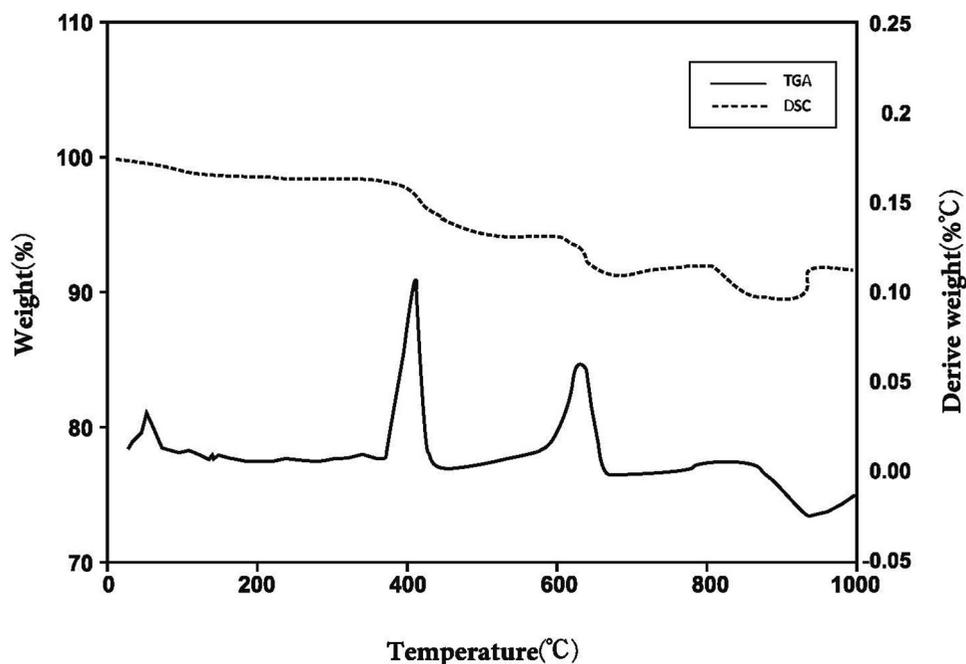**Figure 4.** FE-SEM analysis of St-CDTEA organoclay.



**Figure 5.** Result of the differential thermal analysis of St-CDTEA organoclay.

exchange facilitates the transition of electrons in the St series soil interlayers (Massoudinejad et al. 2019).

### 3.4. Results of FE-SEM analysis

Figures 3–4 show the results of FE-SEM analysis of St series soil and St-CDTEA organoclay, respectively. As shown in Figure 3, the surface structure of St series soil demonstrates a more complex and irregular shape because St series soil contains a higher amount of smectite and its structure contains other mineral structures. Figure 4 shows the structure of St-CDTEA organoclay produced by ion exchange and high-temperature sintering. As shown in the figure, a crystal structure is formed on the surface of the organoclay because it absorbs a significant amount of CDTEA molecules (the molecular structure of CDTEA contains three ethyls) (Guégan 2019), Figure 4 shows that the size of CDTEA molecules transferred to the St-CDTEA organoclay via ion exchange was at the nano-level. This result is backed up by Wei et al. (2009) using modified bentonite clay to examine the feasibility and efficiency of the simultaneous removal of cationic dyes and hydrophobic organic carbons (HOCs) from water (Hou et al. 2018).

### 3.5. The result of TGA analysis

A TGA was adopted for analyzing the rate of weight loss of St-CDTEA organoclay under different temperatures; the results are shown in Figure 5. The aforementioned results in Table 1 indicate St series soil does not have a high organic matter content because it is affected by either rainfall erosion or intensive farming, different properties and trends can be observed through the TGA (Hou et al. 2018; Das et al. 2020; Ma et al. 2019a). For instance, peaks of weight loss occurring at the surface structure of St-CDTEA organoclay were observed when temperatures rose to 50 ~ 100°C, 350 ~ 450°C, 600 ~ 650°C, and 750 ~ 900°C; changes in weight were also more notable under high temperatures (Wu et al. 2016; Sun et al. 2020; Yan et al. 2020). From the results obtained through a TGA, we can say that St-CDTEA organoclay produced from St series soil is characterized by the above-mentioned trends.

### 4. Conclusion

This study finds that St series soil does not have a high organic matter content because it is affected by either rainfall erosion or intensive farming, which causes a decrease in organic matter after it is consumed or lost. Also, the St-CDTEA organoclay has a higher amount of charge because organic matter and free oxides attached to the surface of clay minerals have been removed in the pretreatment process. The results of FT-IR analysis of St-CDTEA organoclay show that factors such as temperature control when synthesizing CDTEA and rate of adding triethylamine can affect the purity of synthesized CDTEA because of its molecular structure contains three ethyls, which in turn affects modification effects. The XRD analysis results indicate that the spacing of layers for St. series soil after it is modified with CDTEA increases. This means that the way in which CDTEA is inserted into the interlayers of clay is double-layered absorption, thereby presenting a double-layered arrangement of St-CDTEA organoclay in said interlayers. The FE-SEM analysis results show that the surface structure of St series soil demonstrates a more complex and irregular shape because St series soil contains a higher amount of smectite and its structure contains other mineral structures. Moreover, the organoclay produced by ion exchange demonstrates a crystal structure after being sintered at 350°C because its surface absorbs a significant amount of CDTEA molecules. These results can be applied to catalytic reactions for pollutants, wherein there are sufficient functional groups to absorb and degrade pollutants.

### Nomenclature

| | |
|---|---|
| CDTEA | Carboxydecyltriethylammonium chloride |
| CEC | Cation exchange capacity |
| FE-SEM | Field emission scanning electron microscope |
| FT-IR | Fourier-transform infrared spectroscopy |
| Santai series soil | (St) series soil |
| TGA | Thermogravimetric analyzer |
| XRD analysis | X-ray diffraction analysis |

### Disclosure statement

No potential conflict of interest was reported by the authors.

### ORCID

Shu-Lung Kuo 🆔 http://orcid.org/0000-0001-7641-4769

### References

Carmody, O., R. L. Frost, J. T. Kloprogge, Y. Xi, and S. Kokot. 2005. "Application of Organo-Clays for Cleaning up Oil Spills." In *13th International Clay Conference*. Tokyo, Japan, 21-27 August 2005: 314-315. Japan: AIPEA.

Carrado, K. A. 2000. "Synthetic Organo- and Polymer-Clays: Preparation, Characterization, and Materials Applications." *Applied Clay Science* 17 (1–2): 1–23. doi:10.1016/S0169-1317(00)00005-3.

Das, R., S. Vupputuri, Q. Hu, Y. Chen, H. Colorado, Z. H. Guo, and Z. Wang. 2020. "Synthesis and Characterization of Antiflammable Vinyl Ester Resin Nanocomposites with Surface Functionalized Nanotitania." *ES Materials and Manufacturing* 8: 46–53. doi:10.30919/esmm5f709.

Doan, L., L. Yang, M. Karatela, V. Phan, C. Jeffryes, T. Benson, and E. K. Wujcik. 2019. "Surface Modifications of Superparamagnetic Iron Oxide Nanoparticles with Polylactic Acid-Polyethylene Glycol Diblock Copolymer and Graphene Oxide for a Protein Delivery Vehicle." *Engineered Science* 7: 10–16. doi:10.30919/es8d510.

Gao, X., X. Zhang, Y. Wang, S. Peng, B. Yue, and C. Fan. 2015. "Rapid Synthesis of Hierarchical BiOCl Microspheres for Efficient Photocatalytic Degradation of Carbamazepine under Simulated Solar Irradiation." *Chemical Engineering Journal* 263: 419–426. doi:10.1016/j.cej.2014.10.110.

Guégan, R. 2019. "Organoclay Applications and Limits in the Environment." *Comptes Rendus Chimie* 22 (2–3): 132–141. doi:10.1016/j.crci.2018.09.004.

He, H. P., R. L. Frost, T. Bostrom, P. Yuan, L. Duong, D. Yang, Y. F. Xi, and T. J. Kloprogge. 2006. "Changes in the Morphology of Organoclays with HDTMA+ Surfactant Loading." *Applied Clay Science* 31 (3–4): 262–271. doi:10.1016/j.clay.2005.10.011.

He, H. P., L. Y. Ma, J. X. Zhu, R. L. Frost, B. K. G. Theng, and F. Bergaya. 2014. "Synthesis of Organoclays: A Critical Review and Some Unresolved Issues." *Applied Clay Science* 100: 22–28. doi:10.1016/j.clay.2014.02.008.

Hou, P., R. Li, Q. Li, N. Lu, K. Wang, M. Liu, X. Cheng, and S. Shah. 2018. "Novel Superhydrophobic Cement-Based Materials Achieved by Construction of Hierarchical Surface Structure with FAS/SiO Hybrid Nanocomposites." *ES Materials & Manufacturing* 1: 57–66. doi:10.30919/esmm5f125.

Kuo, S. L., and E. M. Y. Wu. 2014a. "The Photocatalytical Degradation of Trichloroethylene in Water by Reaction Board Using Clay Catalyst." *Journal of the Indian Chemical Society* 91 (9): 1731–1743.

Kuo, S. L., and E. M. Y. Wu. 2014b. "Adsorption of Cadmium and Aniline of Organoclay by HDTMA and CDTEA Intercalating." *Journal of the Indian Chemical Society* 91 (9): 1757–1763.

Kushwaha, H. S., A. Halder, D. Jain, and R. Vaish. 2015. "Visible Light-Induced Photocatalytic and Antibacterial Activity of Li-Doped $Bi_{0.5}Na_{0.45}K_{0.5}TiO^3$–$BaTiO^3$ Ferroelectric Ceramics." *Journal of Electronic Materials* 44 (11): 4334–4342. doi:10.1007/s11664-015-4007-y.

Li, Q., X. Zhao, J. Yang, C. J. Jia, Z. Jin, and W. Fan. 2015. "Exploring the Effects of Nanocrystal Facet Orientations in g-C3N4/BiOCl Heterostructures on Photocatalytic Performance." *Nanoscale* 7 (45): 18971–18983. doi:10.1039/c5nr05154a.

Li, X., C. Zhu, Y. Song, D. Du, and Y. Lin. 2017. "Solvent Co-Mediated Synthesis of Ultrathin BiOCl Nanosheets with Highly Efficient Visible-Light Photocatalytic Activity." *RSC Advances* 7 (17): 10235–10241. doi:10.1039/C6RA27606G.

Ma, H., J. Shi, X. Y. Zhu, Z. Zhang, J. Li, and S. Cao. 2019a. "AuNRs/Mesoporous Silica/Hydroxyapatite Nanovehicles with Thermally Responsive Polymeric Cap for Remotely Controlled Drug Delivery." *Advanced Composites and Hybrid Materials* 2 (2): 242–253. doi:10.1007/s42114-019-00082-y.

Ma, Y., M. L. Ma, X. Q. Yin, Q. Shao, N. Lu, Y. N. Feng, Y. Lu, et al. 2018. "Tuning Polyaniline Nanostructures via End Group Substitutions and Their Morphology Dependent Electrochemical Performances." *Polymer* 156: 128–135. doi:10.1016/j.polymer.2018.09.051.

Ma, Y., Z. Zhuang, M. L. Ma, Y. Y. Yang, W. T. Li, J. Lin, M. Y. Dong, S. D. Wu, T. Ding, and Z. H. Guo. 2019b. "Solid Polyaniline Dendrites Consisting of High Aspect Ratio Branches Selfassembled Using Sodium Lauryl Sulfonate as Soft Templates: Synthesis and Electrochemical Performance." *Polymer* 182: 121808. doi:10.1016/j.polymer.2019.121808.

Massoudinejad, M., S. M. Mohseni, M. Ghaderpoori, M. Sarkhosh, and S. Sahebi. 2019. "Improvement of Montmorillonite Adsorption Capacity for Lead Ions by Modifying with Hexadecyl Trimethyl Ammonium Chloride: Characterization, Modelling and Optimization Studies." *MethodsX* 6: 2217–2219. doi:10.1016/j.mex.2019.09.032.

Spadavecchia, F., M. Ceotto, L. L. Presti, C. Aieta, I. Biraghi, D. Meroni, S. Ardizzone, and G. Cappelletti. 2014. "Second Generation Nitrogen Doped Titania Nanoparticles: A Comprehensive Electronic and Microstructural Picture." *Chemical Journal of Chemistry* 32 (12): 1195–1213. doi:10.1002/cjoc.201400502.

Sun, M., L. Yuan, X. Yang, and L. Shao. 2020. "Preparation and Modification of Chitosan-Based Membrane." *ES Materials & Manufacturing* 9: 40–47. doi:10.30919/esmm5f780.

Ugochukwu, U. K., and C. I. Fialips. 2017. "Removal of Crude Oil Polycyclic Aromatic Hydrocarbons via Organoclay-Microbe-oil Interactions." *Chemosphere* 174: 28–38. doi:10.1016/j.chemosphere.2017.01.080.

Wei, J. M., R. L. Zhu, J. X. Zhu, F. Ge, P. Yuan, H. P. He, and C. Ming. 2009. "Simultaneous Sorption of Crystal Violet and 2-Naphthol to Bentonite with Different CECs." *Journal of Hazardous Material* 166 (1): 195–199. doi:10.1016/j.jhazmat.2008.11.004.

Wu, M. S., B. Xu, L. Q. Chen, and C. Y. Ouyang. 2016. "Geometry and Fast Diffusion of AlCl4 Cluster Intercalated in Graphite." *Electrochimica Acta* 195: 158–165. doi:10.1016/j.electacta.2016.02.144.

Xi, Y. F., R. L. Frost, H. P. He, T. Kloprogge, and T. Bostrom. 2005a. "Modification of Wyoming Montmorillonite Surfaces Using a Cationic Surfactant." *Langmuir* 21 (19): 8675–8680. doi:10.1021/la051454i.

Xi, Y. W., M. H. He, and R. L. Frost. 2005b. "Thermogravimetric Analysis of Organoclays Intercalated with the Surfactant Octadecyltrimethylammonium Bromide." *Journal of Thermal Analysis and Calorimetry* 81 (1): 91–97. doi:10.1007/s10973-005-0750-2.

Yan, X. R., J. J. Liu, M. Alam Khan, S. Sheriff, S. Vupputuri, R. Das, L. Sun, D. P. Young, and Z. H. Guo. 2020. "Efficient Solvent-Free Microwave Irradiation Synthesis of Highly Conductive Polypropylene Nanocomposites with Lowly Loaded Carbon Nanotubes." *ES Materials & Manufacturing* 9: 21–33. doi:10.30919/esmm5f716.

Yin, Y., B. Jiang, X. F. Zhu, L. H. Meng, and Y. D. Huang. 2019. "Investigation of Thermostability of Modified Graphene Oxide/Methylsilicone Resin Nanocomposites." *Engineered Science* 5: 73–78. doi:10.30919/es8d762.

Zhu, J. X., P. Yuan, H. P. He, R. Frost, Q. Tao, W. Shen, and T. Bostrom. 2008. "In Situ Synthesis of Surfactant/Silane-Modified Hydrotalcites." *Journal of Colloid and Interface Science* 319 (2): 498–504. doi:10.1016/j.jcis.2007.11.037.